Available online at www.sciencedirect.com
ScienceDirect
Computers & Graphics 31 (2007) 668–677
COMPUTERS & GRAPHICS
www.elsevier.com/locate/cag

Chaos and Graphics

A cellular model for three-dimensional snow crystallization

Chen Ning[a], Clifford A. Reiter[b,*]

[a]Faculty of Information and Control Engineering, Shenyang Jianzhu University, Shenyang 110168, China
[b]Department of Mathematics, Lafayette College, Easton, PA 18042, USA

Abstract

Snow crystals are intriguing because they exhibit both symmetry and remarkable diversity. Previous studies have used two-dimensional models to approximate snow crystal growth. Here generalizations to three dimensions are considered. In particular, a cellular arrangement of cells is updated according to local rules that involve the identification of receptive cells and averaging values from non-receptive sites. The cellular arrangement is the same as the configuration of water molecules in ice that occurs under ordinary conditions on Earth.

Keywords: Cellular automata; Ice crystals; Snowflakes

1. Introduction

Snow crystals are fascinating because they have remarkable symmetry while exhibiting diversity that is not easy to explain. However, as early as 1611, Kepler suggested that the symmetry of snow crystals is related to the hexagonal packing of spheres [1], which is remarkably close to being true. Bentley and Humphreys [2], Libbrecht and Rasmussen [3] and Nakaya [4] and many others have photographed thousands of snow crystals giving us a glimpse into their amazing structure. Fig. 1 shows several images from Ref. [2] that illustrate classic six-fold growth although we have little sense of their three-dimensional structure. However, other growth forms, including three-fold symmetric forms, 12-fold symmetric forms, three-dimensional needles and capped columns also appear regularly in naturally occurring snow crystals. A few of these are shown in Fig. 2. A close inspection of the upper right images in Fig. 1 shows that even in figures that appear to have six-fold symmetry at a glance, there may be subtle features that have only three-fold symmetry. Other investigators have studied the physical conditions that lead to particular types of crystal growth. In particular, Nakaya [4] dedicated decades to systematically studying their growth, both in the field and in the laboratory. He found that two parameters were essential in explaining the diversity of snow crystals. For his laboratory experiments, those parameters were air temperature and the temperature of a water bath that introduced water vapor into the air. However, it is usually more convenient to think about air temperature and saturation as the two dominant parameters and those can be correlated to the parameters in his experiments.

Cellular automata are local rules applied to a configuration of cells in a uniform manner. The cells values are usually selected from a finite set of allowed values; however, we will use generalized cellular automata that allow cells to contain real values. Classical applications of cellular automata (some generalized to taking real values) have been made to image processing, image and audio compression and modeling earthquakes, phase transitions, crystal growth, fluid flow, populations, biologic growth and computation [5–12]. It seems reasonable that the three-dimensional growth of snow crystals at a point in space depends largely on the situation in the immediate neighborhood of the point. For cellular models, that corresponds to updating a cell depending upon the state of some local neighborhood of cells. We develop such three-dimensional models in this paper.

Cellular automata on a two-dimensional hexagonal arrangement of cells have been used to simulate snow

*Corresponding author. Fax: +1 610 330 5721.
E-mail addresses: n_chen@126.com (Chen Ning), reiterc@lafayette.edu (C.A. Reiter).

0097-8493/$ - see front matter © 2007 Elsevier Ltd. All rights reserved.
doi:10.1016/j.cag.2007.02.015

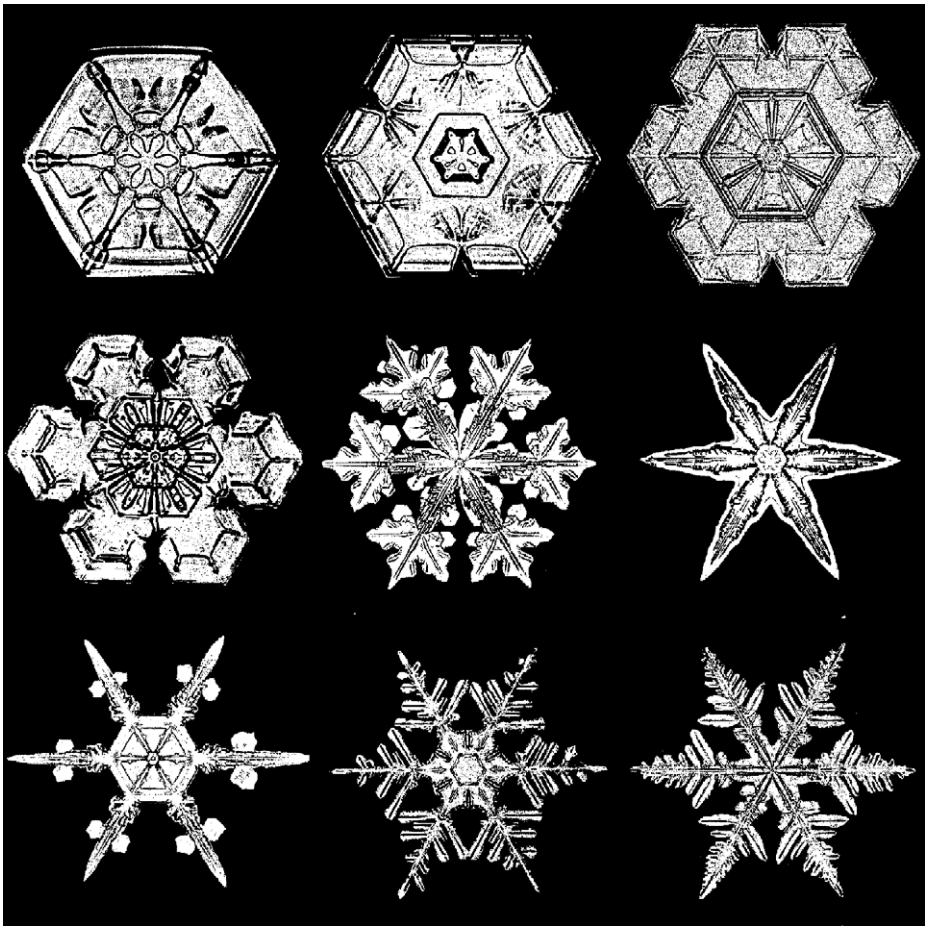

Fig. 1. Some classic six-sided snow crystals.

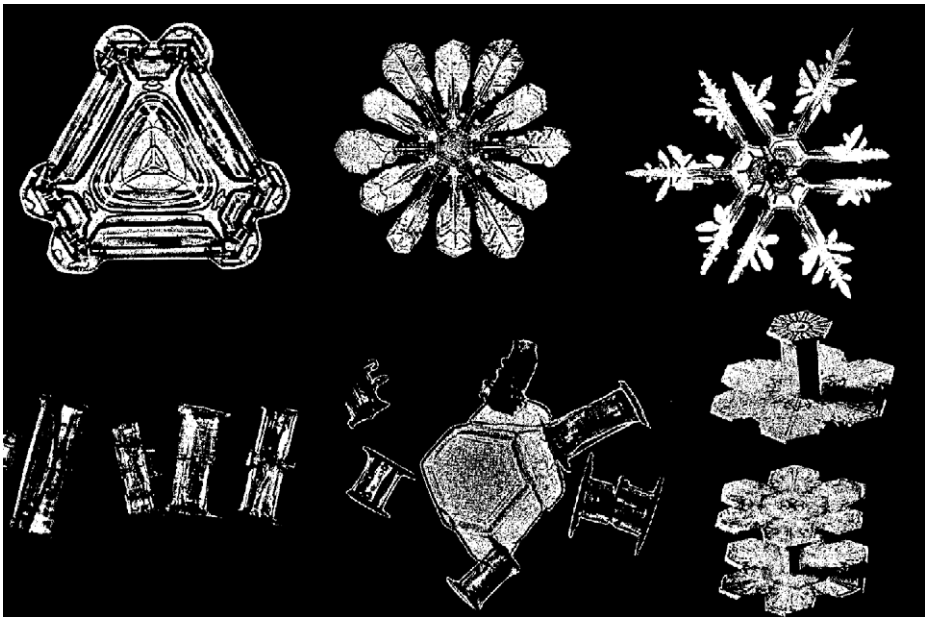

Fig. 2. Some other snow crystals.

crystal growth with perfect six-fold symmetry [13]. Earlier versions of that two-dimensional work appear in Coxe and Reiter [14] and a variation on quasi-crystalline structures appears in [15]. An early paper dealing with cellular snow crystal modeling is [16]. By varying two parameters, the model in [13] led to growth exhibiting stellar, sector, plate

and dendrite patterns. Since that model is two dimensional, it was impossible to model needle growth or capped columns which naturally occur. Fig. 3 shows an example of the growth of dendrites using that two-dimensional model.

This investigation considers cellular growth models in three dimensions. We were motivated by the success of the two-dimensional models and curious to investigate similar models on realistic three-dimensional lattices. In particular, we choose a cellular arrangement that mimics the three-dimensional crystalline structure of ice. We then both generalize and simplify the local rule used in Ref. [13] for this cellular arrangement. We see three-dimensional versions of the growth similar to many of those we saw in two dimensions but new growth forms also appear. In particular, this model exhibits needle growth and growth forms with three-fold symmetry.

Fig. 3. Growth of dendrites from a two-dimensional model.

2. The three-dimensional arrangement of cells

We utilize a cellular arrangement that corresponds to the configuration of the oxygen atoms (the dominant atoms in water molecules) in ordinary ice. While ice crystals with various crystallographic symmetries may be produced in the laboratory, ice occurring naturally at the surface of the Earth is known as Ice-Ih and has the crystallographic structure that we will describe. Detailed descriptions of the structure of ice may be found in [17,18].

Fig. 4a shows a convenient simplified model that we can have as a general model for the arrangement of cells and neighbors. The spheres in the image correspond to water molecules (or the oxygen atoms in ice) and the cylinders correspond to hydrogen bonds between neighboring molecules of ice. The spheres correspond to cells in our cellular configuration and which cells are neighbors are shown with the cylinders. Notice that red cylinders and the cells they connect lie in horizontal planes and form hexagons. These planes are called the basal planes in crystallography. Each cell has three neighbors in the basal plane. We will call these the p-neighbors of the cells. The configuration of cells in each basal plane is replicated in the perpendicular direction. Each cell also has one neighbor in the direction perpendicular to the basal plane. The connections between those neighbors are shown with green cylinders in the figure. Notice that as one moves around a hexagon in a basal plane, the cells alternate between being attached to the basal plane above or below the given plane. This perpendicular direction is called the c-axis direction in crystallography. We will refer to the neighbor in this direction as the q-neighbor.

In actual ice crystals, each cell is tugged slightly out of the basal plane toward its q-neighbor. This results in the configuration of cells as seen in Fig. 4b. We use this configuration for our three-dimensional rendering. However, for purposes of defining our local automata, we need only know that all together, each cell has four neighbors,

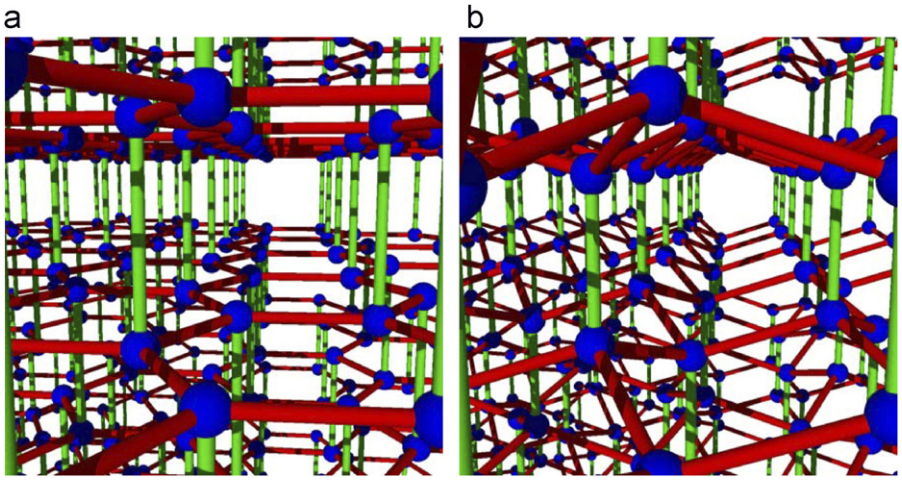

Fig. 4. Cellular arrangement: (a) simple neighbor model and (b) rendering model.

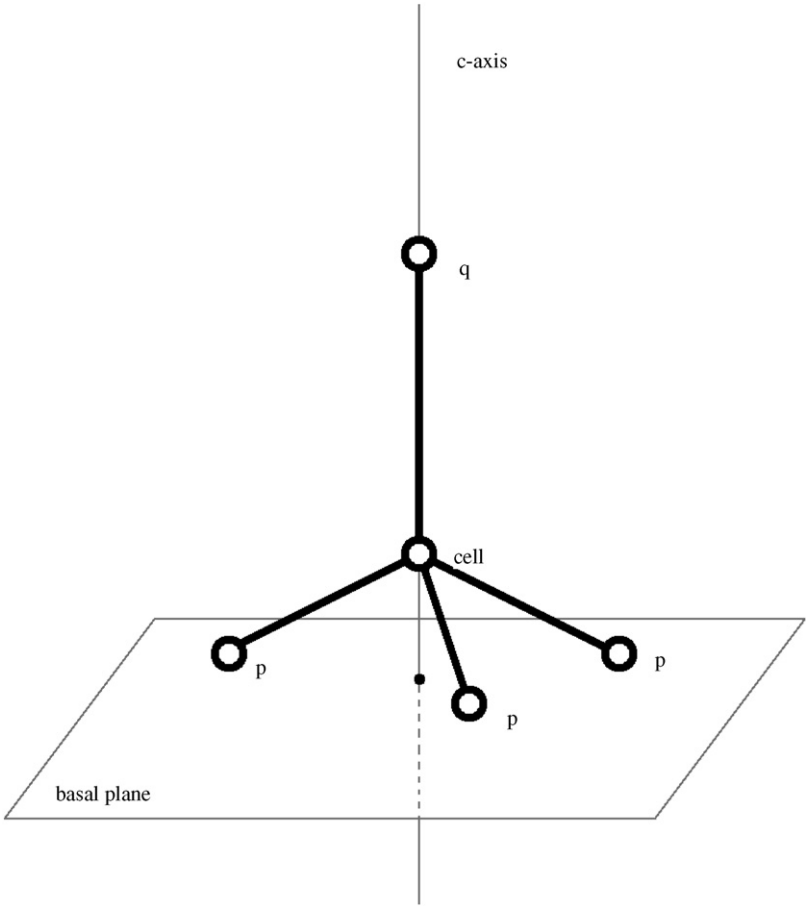

Fig. 5. A simplified view of a cell and its neighbors.

one of them (the q-neighbor) distinguished from the other three. Fig. 5 illustrates that simple neighborhood of a cell. Of course, the global arrangement of these neighborhoods is essential to the global symmetry that we will see develop.

3. The local rule

Before discussing the three-dimensional local rule, we will first describe the rule for the two-dimensional modeling used in [13,15]. The cells each contain a real number between 0 and 1. A cell is considered ice if it has value 1. A cell is called receptive if it is ice or the neighbor of ice. Informally, we consider material at receptive cells to be bound to the ice crystal and non-receptive material to be free to move around. In the two-dimensional models, the values in the cells were split into two hexagonal arrays for further processing before those two arrays were recombined. One of those arrays contained the receptive material with zeros in the non-receptive sites. A constant value, γ, where $0 \leqslant \gamma < 1$, was added to each receptive site, the informal idea being that this accounted for some material being available from the third, un-modeled, dimension. The second array contained the non-receptive values and zeros in the receptive sites. This array was processed by averaging the array. Each cell was replaced by an average of its neighborhood with the center cell having weight one-half and the other cells amounting to the other half. For hexagonal neighborhoods in those two-dimensional models where each cell has six neighbors that meant the six neighbors each had weight $\frac{1}{12}$ in the average. Finally, the two arrays are added together and any excess over 1 removed so that 1 remains the maximal value. That completes one time step of the cellular evolution which is then iterated. For a typical experiment in that two-dimensional work, we seeded a single ice cell as 1 in a uniform field of β values at all the other cells. Descriptions and illustrations of how that model develops may be found in [13]. Fig. 3 shows the result of the evolution of that two-dimensional model from a single ice cell when $\beta = 0.35$ and $\gamma = 0.001$.

For the three-dimensional model we develop here, we also use values between 0 and 1 for our cell values. However, since we now are accounting for all three dimensions, we do not add γ to receptive cells, we simply extend our averaging into the third dimension. We will give the details in the next section. One of our parameters remains the background level. However, to obtain a second parameter, it seems reasonable to bias the averaging weights depending upon whether the neighbors are p-neighbors (from the basal plane) or q-neighbors (in the

perpendicular direction). It turns out that the relative weights of the q-neighbor to those for the p-neighbors is more important than their relative weights compared to the center site. While we will discuss this in further detail later, our primary class of examples is based upon using the same weight at the center site as for the p-neighbors.

4. Variation of primary parameters

As described in Section 2 we are modeling on a cellular arrangement where each cell has four neighbors; namely, three p-neighbors in the basal plane and one q-neighbor in a perpendicular direction. Thus, each neighborhood has five cells when the center is included. As in the two-dimensional case we identify each cell as receptive if the cell or any of its neighbors is ice. The cell is non-receptive otherwise. We split the values in the cells into two arrays. One gives the values at receptive sites (0 elsewhere). Unlike the two-dimensional case, no further processing (i.e., no added gamma) is done to this array of receptive values. The second array contains the values at the non-receptive sites (0 elsewhere). This array is processed by averaging over the neighborhoods. The non-ice receptive sites will typically receive a non-zero value from this averaging. The weights used in the averaging will vary, but always sum to 1. In this section we will take the center weight to be the same as that for the p-neighbors and hence we can specify the averaging scheme by giving the ratio, r, of the weight for the q-neighbor to that for the p-neighbors. In particular, when $r = 1$, the weights used for all five cells are $\frac{1}{5}$ while when $r = 2$, the weights used for the center and p-neighbors are all $\frac{1}{6}$ and the q-neighbor takes the weight $\frac{2}{6}$. Fig. 6 shows an example of a small cellular patch being updated so that a receptive cell becomes ice. While there is not enough data visible to verify the particular computation, it is illustrative of the general scheme being used.

Fig. 7 illustrates the result of growth of our model for various r and β values. The size of the arrangement of cells was $150 \times 150 \times 150$. A single central cell was turned to ice and evolution ceased when ice reached within three cells of a boundary or if the number of iterations exceeded 5000. Color corresponds to position with z-position dominating the change when that is feasible. In any case, the color adds redundant information, but helps the interpretation of information lost by the projection of the three-dimensional model into a planar image. The cells are configured as in Fig. 4b and ice produced by our automata is rendered using overlapping spheres in the raytracing program POVRay [19]. While the individual spheres are visible, they have been somewhat blended together using POVRay's blob type.

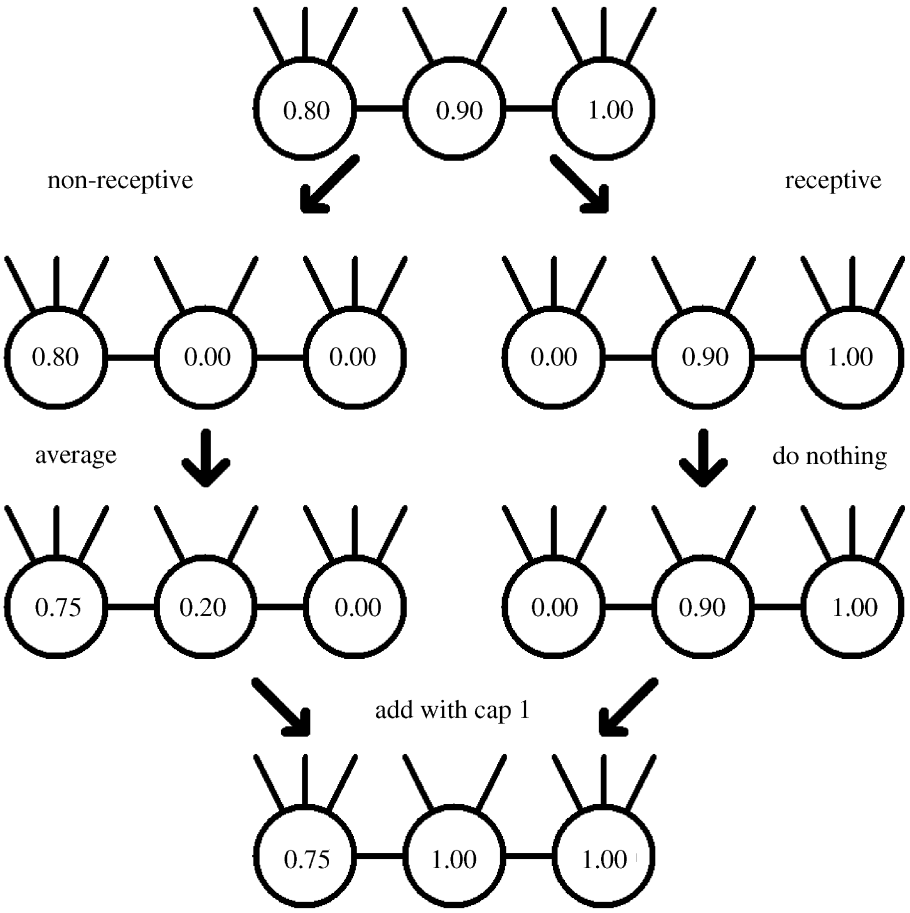

Fig. 6. The scheme used for updating cells illustrating a receptive cell becoming ice.

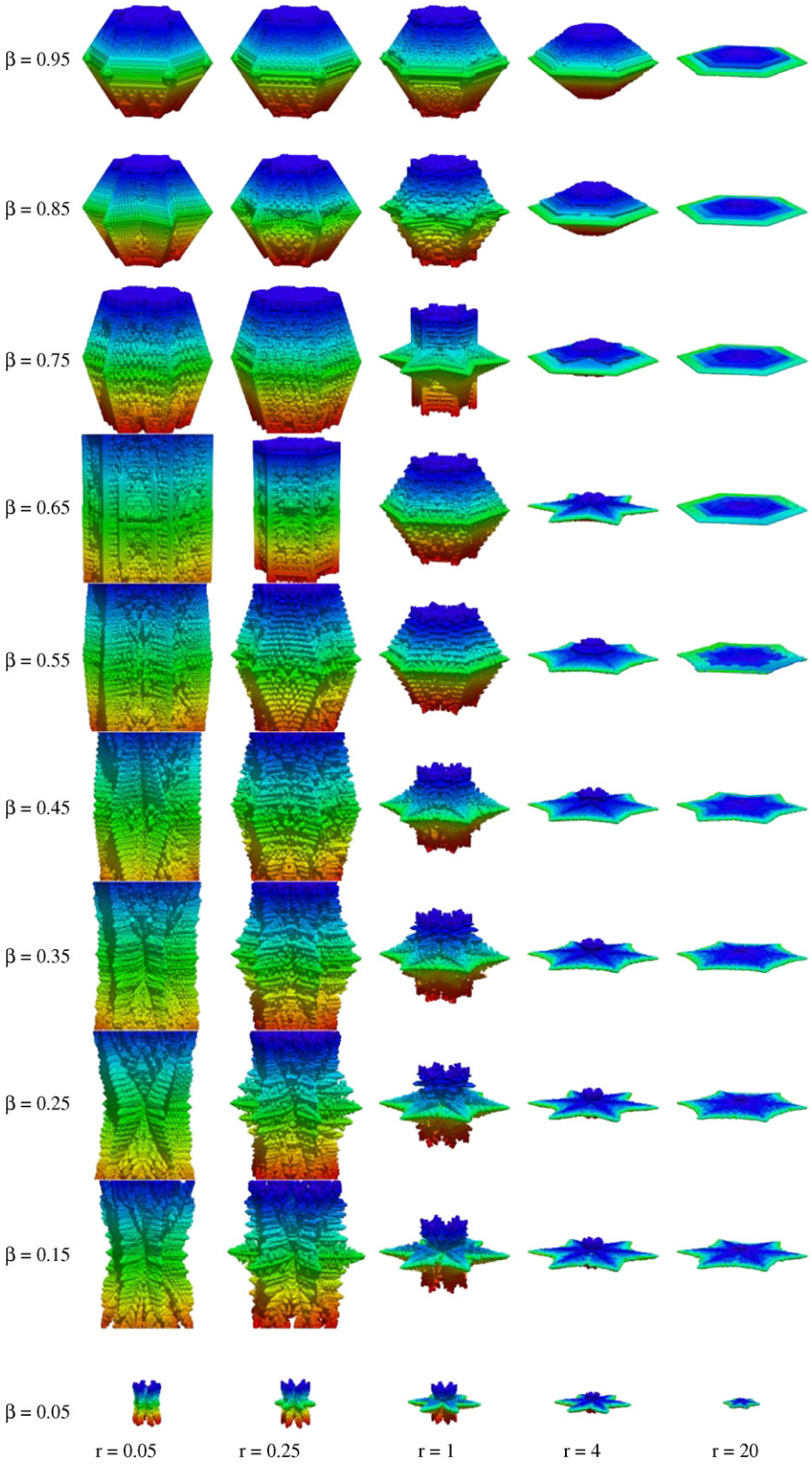

Fig. 7. Sample growth as β and r vary; side view.

Fig. 7 uses a view from the side so that the c-axis is vertical in the figure. In the figure, we see that small values of r tend to produce long crystals with c-axis direction growth significant, while large values of r produce more planar growth. For r larger than 1, we see that as β increases, growth changes from dendrites toward stellar and hexagonal plate forms. In Fig. 8, we consider the same variation of r and β values with view nearly straight down

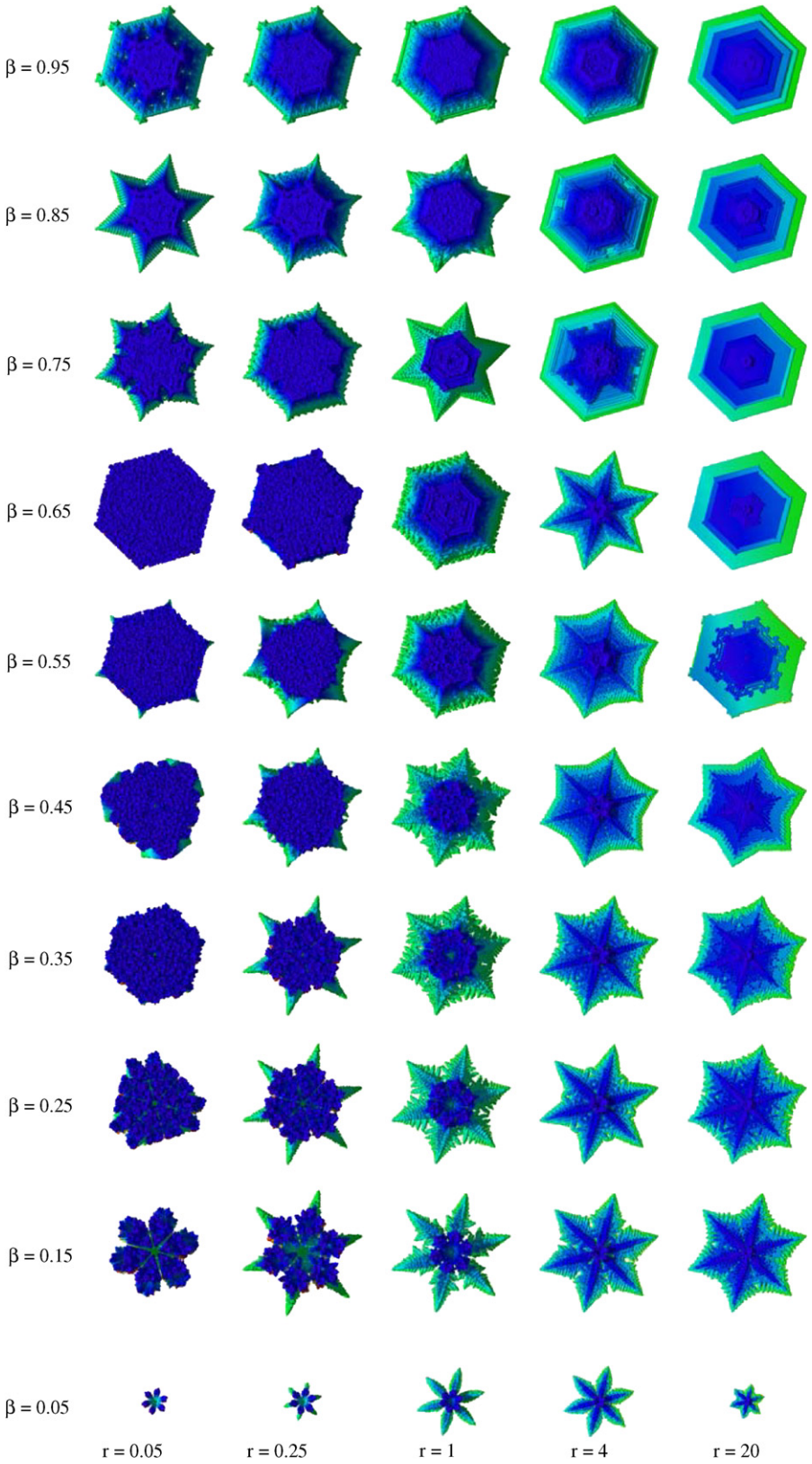

Fig. 8. Sample growth as β and r vary; top view.

the c-axis. Here the changes from dendrites toward stellar and hexagonal plate forms are even more apparent. The variety of cross-sectional forms for the columnar growth (smaller r values) is easy to observe. Note also that several of these forms have (like some of the growth in Fig. 2) very obvious three-fold (but not six-fold) symmetry. For

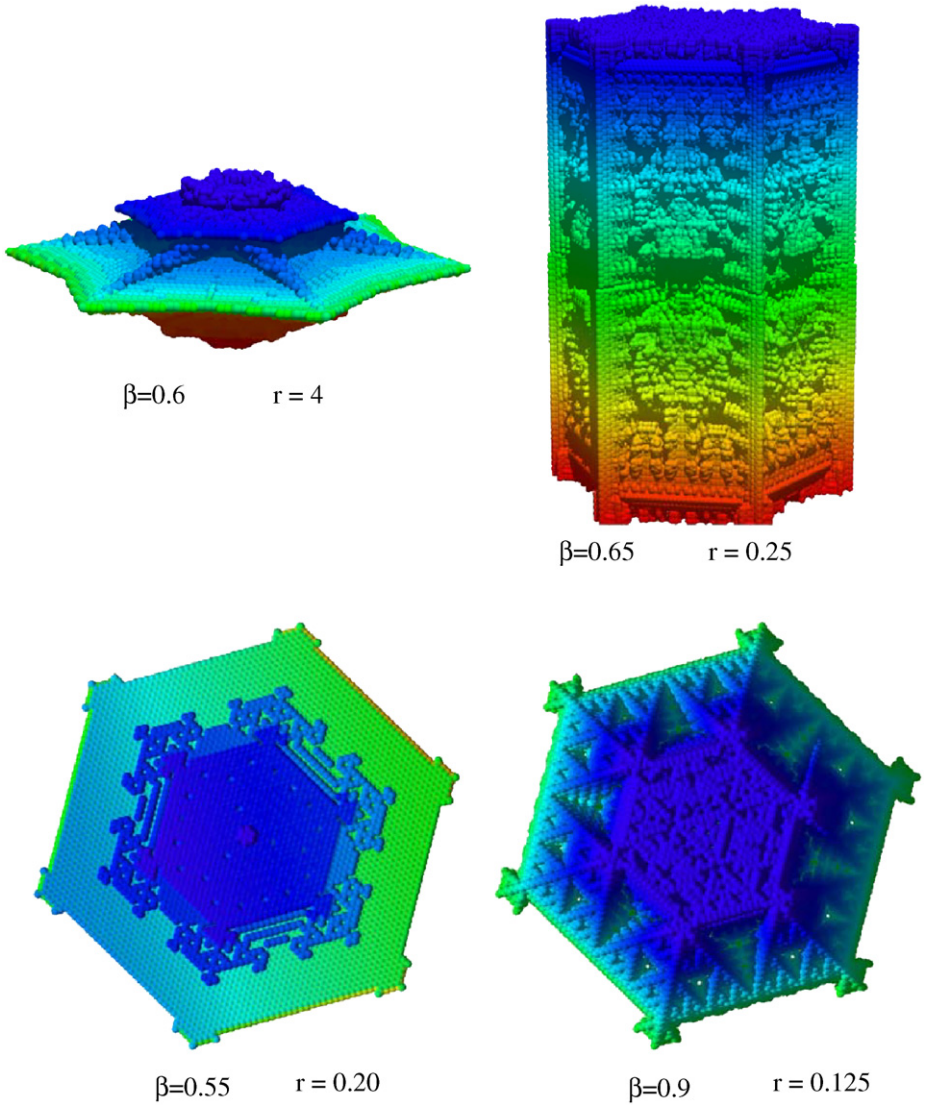

Fig. 9. Some more detailed views.

example, $r = 0.05$, $\beta = 0.25$. Also notice that some of the columns have "waists" as do some of the columnar forms in Fig. 2.

Fig. 9 shows some of the examples from Figs. 7 and 8 in more detail. The capped plates in Fig. 2 would seem to result from a change in growing conditions: from columnar growth to plate growth. Notice that when $\beta = 0.6$ and $r = 4$ two horizontal plates appear to be the dominant growth patterns (and a third plate is barely visible). Thus, our model comes close to producing features like capped columns even without changing the growth conditions. When $\beta = 0.65$ and $r = 0.25$, we see a column grow with remarkable vertical uniformity. When $\beta = 0.55$ and $r = 20$ we see some subtle three-fold symmetric features reminiscent of the snowflakes in the upper right of Fig. 1. When $\beta = 0.9$ and $r = 0.125$ we see an almost fractal pattern of growth although the overall extent is closer to a ball in the sense that the growth is similar in the basal and c-axis directions. These fractal structures appear for relatively low r and high β. They do not seem to be a common form of naturally occurring snow crystal although rough sphere-like snow grapple is a common form of snow and similar growth occurred for the analogous two-dimensional models [13]. More detailed illustrations resulting from this type of growth for additional r and β values appears at [20].

5. Variations

Next we consider the situation where we vary the averaging weight associated with the center cell. Suppose we take the p-neighbors and q-neighbors to have the same weight. Let s denote the ratio of the weight for the center cell to the weight of the other cells. Fig. 10 shows the result of using $s = 0.25$, 1 and 4 when $\beta = 0.15$. Notice that these all are similar to images that were seen in Figs. 7 and 8; this is consistent with our experience that by varying the ratio r as in the previous section, we see the same qualitative behaviors.

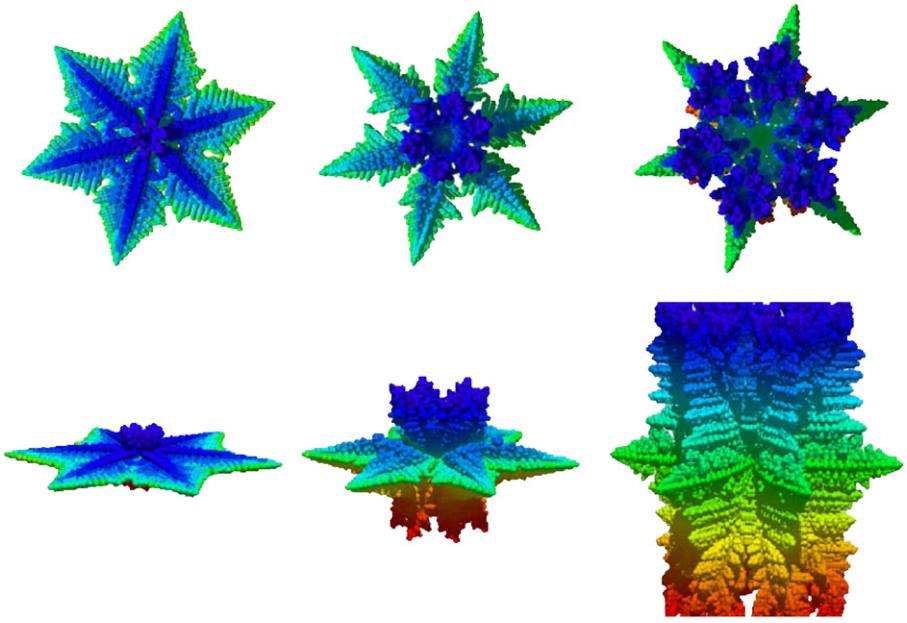

Fig. 10. Varying the center weight for averaging for $s = 0.25$, 1 and 4 with $\beta = 0.15$ has little impact on the qualitative growth forms.

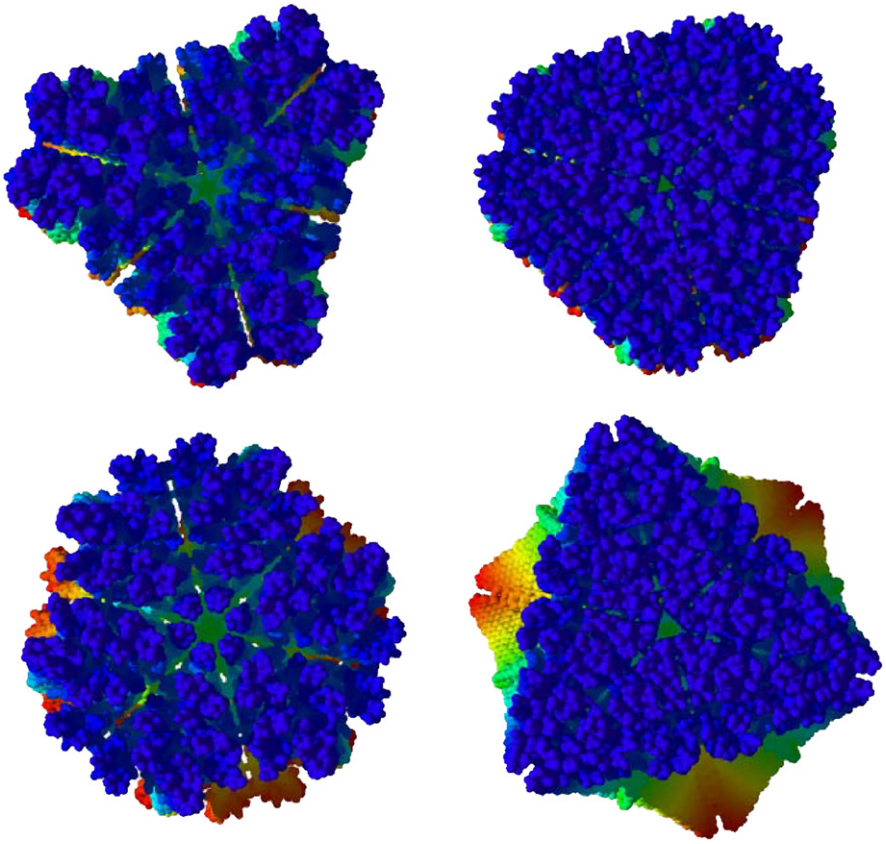

Fig. 11. Changing the initial ice configuration from a single cell (top row) to six cells (bottom row) forming a hexagon for $r = 0.05$ and $\beta = 0.2$, 0.3.

In Figs. 8 and 9, we see examples where three-fold symmetry is apparent. We next show the result of comparing $r = 0.05$ with $\beta = 0.2$ and 0.3 growth with different initial conditions. The top images in Fig. 11 show the result of those experiments with the usual single initial cell of ice. The bottom images in the figure show the corresponding growth when six cells forming a hexagon are initially ice. Notice that there is more six-fold symmetry in the projection, but that in three dimensions the result may still be strongly three-fold, as seen in the bottom right

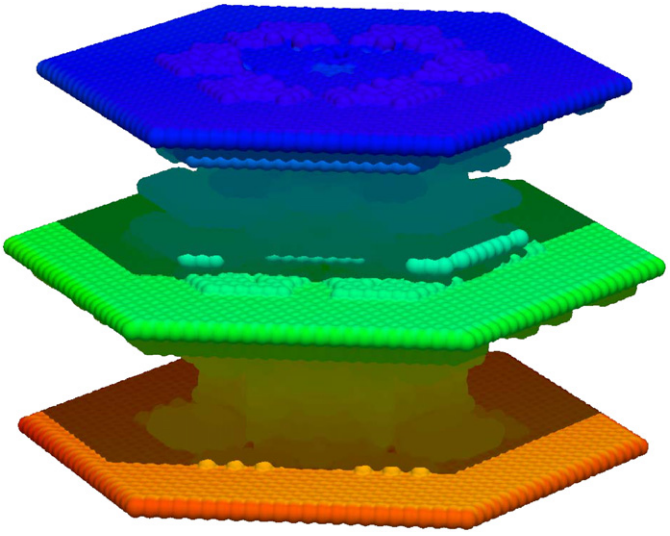

Fig. 12. Capped columns resulting from changing from $r = 0.25$ to $r = 20$ for $\beta = 0.65$.

where the red corresponds to portions of the growth that are at the bottom. These experiments illustrate the great sensitivity of these growth models.

Fig. 12 shows the result of running $r = 0.25$ with $\beta = 0.65$ on a single initial ice cell followed by 30 steps of $r = 20$ with β remaining unchanged. Notice the dramatic capped columns with three primary levels. Similar capped columns appear in Fig. 2.

6. Concluding remarks

The model presented here provides a simple rule for updating a three-dimensional configuration of cells in order to model snow crystal growth. This model is deterministic and utilizes only two parameters. We see examples of dendrite, stellar and plate growth commonly seen in nature and also seen in previous two-dimensional models. This three-dimensional model exhibits new types of growth, including three-fold symmetric growth, columnar and capped columnar growth. Our model could be made more physical by demanding conservation of mass, for example. However, our efforts in that direction lead to periodic configurations that frustrated robust model design. In the many cases where such models exhibited growth, the growth had grainy feel, like often seen in diffusion-limited growth models. Averaging could be used to remove that graininess. However, in our model, averaging is used both for smoothing and transport and we believe that this allows for such a simple model to successfully model so many different types of three-dimensional snow crystal growth.

Acknowledgments

This work was accomplished while Professor Chen Ning was a visiting scholar at Lafayette College. The support Natural Science Foundation of Liaoning province of China (20032005) and the Foundation of Science and Technology Bureau of Shenyang (200143-01) and the hospitality of Lafayette College are greatly appreciated.

References

[1] Kepler J. The six sided snowflake (1611): translation. Oxford: Oxford University Press; 1966.
[2] Bentley WA, Humphreys WJ. Snow crystals. McGraw-Hill Book Company, 1931 [Also, New York: Dover Publications; 1962].
[3] Libbrecht K, Rasmussen P. The snowflake: winter's secret beauty. Stillwater: Voyageur Press; 2003 Auxiliary: http://www.snowcrystals.com.
[4] Nakaya U. Snow crystals: natural and artificial. Cambridge, MA: Harvard University Press; 1954.
[5] Chopard B, Droz M. Cellular automata modeling of physical systems. New York: Cambridge University Press; 1998.
[6] Gaylord R, Nishidate K. Modeling nature: cellular automata simulations with mathematica®. New York: Springer; 1996.
[7] Goles E, Martínez S, editors. Cellular automata and complex systems. Dordrecht: Kluwer Academic Publishers; 1999.
[8] Griffeath D, Moore C, editors. New constructions in cellular automata. New York: Oxford University; 2003.
[9] Ilachinski A. Cellular automata: a discrete universe. Singapore: World Scientific; 2001.
[10] Russ JC. The image processing handbook, 4th ed. Boca Raton, FL: CRC Press; 2002.
[11] Wolfram S. A new kind of science. Champaign: Wolfram Media; 2002.
[12] Wolf-Gradow DA. Lattice-gas cellular automata and lattice Boltzmann models. Berlin: Springer; 2000.
[13] Reiter CA. A local cellular model for snow crystal growth. Chaos, Solutions and Fractals 2005;23:1111–9.
[14] Coxe AM, Reiter CA. Fuzzy hexagonal automata and snowflakes. Computers and Graphics 2003;27:447–54.
[15] Chidyagwai P, Reiter CA. A local cellular model for growth on quasicrystals. Chaos, Solutions and Fractals 2005;24:803–12 Auxiliary materials http://www.lafayette.edu/~reiterc/mvp/qcgm/index.html.
[16] Packard NH. Lattice models for solidification and aggregation. In: Wolfram S, editor. Theory and applications of cellular automata. Singapore: World Scientific Publishing; 1986. p. 305–10.
[17] Petrenko V, Whitworth R. The physics of ice. New York: Oxford University Press; 1999.
[18] Pounder ER. The physics of ice. Oxford: Pergamon Press; 1965.
[19] PovRay 3.5. Persistence of vision Raytracer. 〈http://www.povray.org〉.
[20] Chen N, Reiter CA. Auxiliary materials for a cellular model for 3-dimensional snow crystallization. 〈http://www.lafayette.edu/~reiterc/mvq/3d_snow/index.html〉.